Bol. Soc. Paran. Mat.
©SPM – E-ISSN-2175-1188
SPM: www.spm.uem.br/bspm

(3s.) **v. 2025 (43) 1** : 1–18.
ISSN-0037-8712
doi:10.5269/bspm.75426

Impact of the diffusion coefficient and non-linear incidence rate on the dynamics of the SIR model

Kuldeep Malik, Pranay Goswami* and Vikash Yadav

ABSTRACT: This paper proposes a Susceptible-Infected–Recovered (SIR) mathematical model with diffusion coefficient. Nonlinear incidence and treatment rates are employed to control infectious diseases and epidemics. In this study, the treatment rate is regarded as Holling type II function, while the infection incidence rate is viewed as Crowley–Martin type function. A detailed mathematical analysis is carried out that includes non-negativity and existence of solution, existence of both type disease free and endemic equilibrium points. Further, stability analysis at equilibrium points is performed. Additionally, the numerical simulation is conducted and graphical representations are displayed. The results show the impact of diffusion coefficients and non-linear incident and recovery rates on susceptible, infected and recovered populations.

Key Words: Existence of Equilibrium Points, Numerical simulation, SIR model with non-linear incident and recovery rate, Stability analysis at equilibrium.

Contents

1. Introduction

Mathematical modeling plays a crucial role in various scientific disciplines, including physics, biology, earth science, and chemistry, as well as in engineering fields such as computational science and electrical engineering. One field that utilizes mathematical modeling to forecast the spread of infectious diseases is epidemiology, a vital area of study in population biology with applications in public health. An epidemic is characterized as an unexpected disease outbreak that causes significant harm to a large proportion of the population before it can be controlled. Several years can pass between pandemic outbreaks before they reoccur. Epidemiology is the study of disease occurrence. The widespread transmission of infectious diseases affects millions of people and negatively impacts the economic, political, social, and geographic aspects of society. Cholera, malaria, and other infectious diseases are considered endemic in many countries worldwide. Some diseases, like influenza, are caused by viruses; others, like tuberculosis, are caused by bacteria; while others, like malaria, are spread by vectors such as flies, ticks, and mosquitoes. Epidemiological models are crucial tools for understanding the factors influencing the rise and fall of infectious diseases. Mathematical modeling is particularly useful when obtaining information through direct observation or experimentation is not feasible. It aids in comprehending the mechanisms

* Corresponding author
2010 *Mathematics Subject Classification:* 26A33, 92B05, 92C60.
Submitted January 28, 2025. Published June 24, 2025

of disease transmission. For a better understanding of epidemiological models, as well as infection control and prevention strategies, mathematical modeling of infectious disease transmission is essential. It provides both short- and long-term predictions of disease occurrence in the general population while accounting for multiple influencing factors.

Numerous mathematical models have been presented in the literature on epidemic modelling to restrict the transmission of disease, including SIS [5,3], SIR [13,16,17,20], $SEIR$ [19,8,22], $SVEIR$ [10], $SIRS$ [30,1], and several more. The aforementioned models comprise systems of ordinary differential equations ODE or Partial differential equations (PDE) and rely primarily on compartmental analysis. These compartments are identified as the susceptible population (S), the infected population (I), and the recovered population (R). Infection, progression, healing, or migration are the factors that drive movement across these compartments. These variables display the total number of people in each section at any given time. In this case, S represents the total count of susceptible persons. When a susceptible individual encounters an infected individual, they contract the illness and become a member of the infected group. I represents the overall number of infected individuals. They are contagious and can spread to vulnerable groups R is the share of recovered immune people. The SIR model, put forth by W.O. Kermack and A.G. McKendrick in 1927, was essential to mathematical epidemiology [14]. In subsequent work, Kermack and McKendrick (1932) first included the consequences of considerable dynamics [15]. H.W. Hethcote summarised the model's applications in 1976 [12]. All of the human population is represented by $N = S + I + R$, where N is kept constant throughout the simulation. The following is the model put forth by Kermack and Mckendrick in 1927:

$$\begin{cases} \dfrac{dS}{dt} = -\beta SI, \\ \dfrac{dI}{dt} = \beta SI - \alpha I, \\ \dfrac{dI}{dt} = \alpha I. \end{cases} \tag{1.1}$$

Where β and α stand for the infection and recovery rates of the infected individuals, respectively.

In the literature, many different models of epidemics have been put forth to control the disease spread. Interventions such as treatment, immunisation, quarantine, and many more are crucial in epidemiology because they aid in preventing the spread of illness. Numerous researchers have used various treatment functions to examine the effects of treatment. An effective and prompt treatment approach can significantly lessen the impact of illness on society. The rate of treatment of infectious persons is thought either to be constant or proportionate to the count of infected people in traditional epidemic models. Nonetheless, we are aware that the community's resources for treatment are scarce. As a result, selecting an appropriate disease treatment rate is crucial. The tactics for controlling epidemics in the absence of feasible therapeutic treatments and vaccinations rely on adopting suitable preventive measures. The following describes a SIR epidemic model that Wang and Ruan [28] examined in 2004 with a treatment rate of constant (i.e., the recovery from infected subgroup per unit time)

$$H(I) = \begin{cases} b, & I > 0 \\ 0, & I = 0 \end{cases}, \tag{1.2}$$

with a positive constant b and share of infected people I. They demonstrated that this model displays a variety of bifurcations by performing stability analysis. An enhanced treatment rate was also covered by Zhang and Liu [32] and is represented by the continuous differentiable function below, which saturates at a maximum value:

$$H(I) = \frac{aI}{1+bI},\ a \geq 0,\ b \geq 0,\ I \geq 0, \tag{1.3}$$

where the cure rate is indicated by the positive constant a and the treatment availability constraint is measured by the non-negative constant b. Recently, Zhang et al. [33], Dubey et al. [8] and Zhou et al. [34] investigated this nonlinear saturation treatment rate in a somewhat distinct manner. Holling type II is another name for the used nonlinear treatment rate.

It is well known that the incidence rate is crucial for controlling and simulating the dynamics of an epidemic. A number of researchers have recently focused on nonlinear type incidence rates [16,17,25,2], although the incidence rate was characterised as bilinear in standard models. Despite being based on the law of mass action, the bilinear incidence rate used in the literature is irrational for large populations. Researchers have taken into account a variety of nonlinear incidence rate types [8,18,31,21], including Beddington–DeAngelis type, Holling type II and many more, to comprehend the underlying dynamics of infectious diseases. Thus, incorporating the aforementioned elements, we suggest a mathematical model for SIR epidemics by utilising an incidence rate of the Crowley-Martin type, which is described as

$$\frac{\beta SI}{(1+\theta_1 S)\,(1+\theta_2 I)}. \tag{1.4}$$

In 1989, P. H. Crowley and E. K. Martin first presented this functional response [7,24]. At time t, the term $\frac{\beta SI}{(1+\theta_1 S)(1+\theta_2 I)}$ denotes the ratio by which a susceptible person departs from the susceptible category and subsequently joins the infectious category. Even when susceptible populations are highly concentrated, the incidence rate of Crowley-Martin type normalises the inhibition impact on infectious agents [9]. This is evident in the following way:

$$\lim_{S\to\infty} \frac{\beta SI}{(1+\theta_1 S)\,(1+\theta_2 I)} = \frac{\beta I}{\theta_1\,(1+\theta_2 I)}. \tag{1.5}$$

More general kinds of realistic models result from models where the transfer rates are dependent on compartment sizes both at the time of transfer and in the past. Diffusion has a substantial impact on the mechanisms of epidemic and it profoundly affects model outcomes. Thus, the current study intends to investigate the influence of diffusion on the epidemic model in which the incidence rate of Crowley-Martin establishes the progression of infection in individuals while the rate of treatment as Holling type II, which creates programs for the management of illness and disease in human population. An extended version of the SIR epidemic model, known as the SIR reaction-diffusion model, is examined both qualitatively and quantitatively in this work. Additionally, by using Crowley–Martin incidence rate and recovery rate as a Holling type II, the study is connected with the availability of resources, such as numbers of beds in hospitals, oxygen cylinders, or dosages of vaccines, depending on the disease being studied. The purpose of this research is to solve the epidemic model numerically to aid in the disease's geographical spread in a community that has not received the vaccination, as well as to look into how the reaction-diffusion system behaves asymptotically.

The SIR reaction–diffusion model can be explained by choosing η, boundary's outward unit normal vector and Ψ, bounded domain in $\mathbb{R}^n$ with a smooth boundary $\partial\Psi$ and is described as

$$\begin{cases} S_t - \tau_1 \Delta S = (1-\rho)\delta N - \dfrac{\beta SI}{(1+\theta_1 S)(1+\theta_2 I)} - \mu S, \\ I_t - \tau_2 \Delta I = \dfrac{\beta SI}{(1+\theta_1 S)(1+\theta_2 I)} - \dfrac{\lambda_1 I}{1+\lambda_2 I} - (\mu+\vartheta+\pi) I, \\ R_t - \tau_3 \Delta R = \dfrac{\lambda_1 I}{1+\lambda_2 I} + \pi I + \rho\delta N - \mu R, \end{cases} \tag{1.6}$$

subject to homogeneous Neumann boundary restrictions

$$\partial_\eta S = \partial_\eta I = \partial_\eta R = 0,\ \omega \in \partial\Psi,\ t > 0,$$

and the initial conditions

$$\begin{aligned} S(\omega,0) &= S_0 = \exp\left(-\left(\frac{\omega}{1.4}\right)\right) * 0.86,\ \omega \in \bar{\Psi}, \\ I(\omega,0) &= I_0 = \exp\left(-\omega^2\right) * 0.04,\ \omega \in \bar{\Psi}, \\ R(\omega,0) &= R_0 = N - S_0 - I_0, \end{aligned}$$

with the parameters stated as

- $S(\omega,t)$- the susceptible population where ω occupies space and time t,
- $I(\omega,t)$- the infected population where ω occupies space and time t,
- $R(\omega,t)$- the recovered population where ω occupies space and time t,
- τ_1- the diffusion coefficient for the susceptible individuals,
- τ_2- the diffusion coefficient of the infected population,
- τ_3- the diffusion coefficient of the recovered individuals,
- ρ- the ratio of vaccination,
- δ- the rate of natural births,
- N- total population,
- β- the rate of infection,
- θ_1- the degree of inhibition taken by susceptible population,
- θ_2- the degree of inhibition taken by infected population,
- μ- the rate of natural morality,
- ϑ- the diseased induced morality rate,
- λ_1- the rate of cure,
- λ_2- the limiting rate in resource availability,
- π- the natural rate of recovery.

2. Mathematical Analysis

2.1. Non-negativity, existence and uniqueness of solution

Consider the system

$$\begin{cases} S_t - \tau_1 \Delta S = (1-\rho)\delta N - \dfrac{\beta SI}{(1+\theta_1 S)(1+\theta_2 I)} - \mu S, \\ I_t - \tau_2 \Delta I = \dfrac{\beta SI}{(1+\theta_1 S)(1+\theta_2 I)} - \dfrac{\lambda_1 I}{1+\lambda_2 I} - (\mu+\vartheta+\pi)I, \\ R_t - \tau_3 \Delta R = \dfrac{\lambda_1 I}{1+\lambda_2 I} + \pi I + \rho\delta N - \mu R, \end{cases}$$

in addition to homogeneous Neumann boundary restrictions

$$\partial_\eta S = \partial_\eta I = \partial_\eta R = 0,\ \omega \in \partial\Psi,\ t > 0,$$

and the initial conditions are

$$\begin{aligned} S(\omega,0) &= S_0 = \exp\left(-\left(\frac{\omega}{1.4}\right)\right) * 0.86,\ \omega \in \bar{\Psi}, \\ I(\omega,0) &= I_0 = \exp\left(-\omega^2\right) * 0.04,\ \omega \in \bar{\Psi}, \\ R(\omega,0) &= R_0 = N - S_0 - I_0. \end{aligned}$$

According to the maximum principle [23], for $\omega \in \bar{\Psi}$ and $t \in (0, \Gamma_{\max})$, where $\Gamma_{\max}$ is the longest period of time that the system (1.6) solutions exist, all the compartments $S(\omega,t)$, $I(\omega,t)$, and $R(\omega,t)$ are non-negative. Also all $S(\omega,t)$, $I(\omega,t)$, and $R(\omega,t)$ are bounded over $\bar{\Psi} \times (0, \Gamma_{\max})$. Therefore, with the same

approach as of [11] and by the conventional approach to semilinear parabolic systems it can be derived that $\Gamma_{\max} = \infty$ and the system (1.6) has unique classical solution $S(\omega, t)$, $I(\omega, t)$, and $R(\omega, t)$ for whole time-space. Now by the method applied in [4] the overall count of people in Ψ at $t = 0$ is

$$N = \int_{\Psi} [S(\omega, 0) + I(\omega, 0) + R(\omega, 0)]\, d\omega > 0, \text{ for all } t > 0.$$

By adding all three equations in (1.6) and applying integration over Ψ, we get

$$\frac{\partial}{\partial t} \int_{\Psi} [S + I + R]\, d\omega = \int_{\Psi} [\tau_1 \Delta S + \tau_2 \Delta I + \tau_3 \Delta R]\, d\omega = 0,$$

suggests that the population's overall size is constant and should be treated as N for the purposes of the study. The impact of R is absent from the first two equations of model (1.6). Hence the system (1.6) can be reduced as

$$\begin{cases} S_t - \tau_1 \Delta S = (1-\rho)\delta N - \dfrac{\beta SI}{(1+\theta_1 S)(1+\theta_2 I)} - \mu S, \\ I_t - \tau_2 \Delta I = \dfrac{\beta SI}{(1+\theta_1 S)(1+\theta_2 I)} - \dfrac{\lambda_1 I}{1+\lambda_2 I} - (\mu + \vartheta + \pi) I, \end{cases} \tag{2.1}$$

with R can be determined by $R(\omega, t) = N - S(\omega, t) - I(\omega, t)$. The reduced model will be used for subsequent mathematical analysis.

2.2. Disease free equilibrium(DFE)

The method described in [26] will be used to determine whether equilibrium points exist and to perform a stability study at equilibrium points for system (2.1). Consider the system

$$\begin{cases} S_t - \tau_1 \Delta S = (1-\rho)\delta N - \dfrac{\beta SI}{(1+\theta_1 S)(1+\theta_2 I)} - \mu S, \\ I_t - \tau_2 \Delta I = \dfrac{\beta SI}{(1+\theta_1 S)(1+\theta_2 I)} - \dfrac{\lambda_1 I}{1+\lambda_2 I} - (\mu + \vartheta + \pi) I. \end{cases}$$

To determine equilibrium points, we need to solve

$$\begin{cases} (1-\rho)\delta N - \dfrac{\beta SI}{(1+\theta_1 S)(1+\theta_2 I)} - \mu S = 0, \\ \dfrac{\beta SI}{(1+\theta_1 S)(1+\theta_2 I)} - \dfrac{\lambda_1 I}{1+\lambda_2 I} - (\mu + \vartheta + \pi) I = 0. \end{cases} \tag{2.2}$$

The aforementioned system needs to be solved for $I = 0$ in order to achieve disease-free equilibrium points. Hence

$$(1-\rho)\delta N - \mu S = 0,$$

implies, the unique DFE is $E_0 \left(\frac{(1-\rho)\delta N}{\mu}, 0 \right)$ or say $E_0 \left(\frac{B}{\mu}, 0 \right)$ with $B = (1-\rho)\delta N$.

2.3. Basic reproduction number

The average number of subsequent infections that an infected person produces throughout their infected phase when they are placed in a completely susceptible community is known as the basic reproduction number. The basic reproduction number, denoted by $\Re_0$, will be ascertained using the next-generation matrix technique methodology [27]. On comparing 2.1 with [27], it is obtained

$$f = \frac{\beta SI}{(1+\theta_1 S)(1+\theta_2 I)}$$

,

$$v = \frac{\lambda_1 I}{1+\lambda_2 I} + (\mu + \vartheta + \pi) I$$

. The partial derivative will now be used to evaluate F and V at the equilibrium point free from disease, which is

$$F = \left.\frac{\partial f}{\partial I}\right|_{E_0}, \; V = \left.\frac{\partial v}{\partial I}\right|_{E_0},$$

implies

$$F = \left[\frac{\beta S}{(1+\theta_1 S)}\right]_{S=\frac{B}{\mu}},$$

$$V = \left[\lambda_1 + (\mu + \vartheta + \pi)\right]_{S=\frac{B}{\mu}},$$

and $\Re_0$ will be the spectral radius of FV^{-1}, hence

$$\Re_0 = \frac{\beta(1-\rho)\delta N}{(\mu+\theta_1(1-\rho)\delta N)\,(\lambda_1+\mu+\vartheta+\pi)} = \frac{\beta B}{(\mu+\theta_1 B)\,(\lambda_1+\mu+\vartheta+\pi)}. \tag{2.3}$$

2.4. Endemic equilibrium(EE)

For the endemic equilibrium $E = \left(S^{\#}, I^{\#}\right)$, we may rewrite the system (2.2) equations for the endemic equilibrium points $S^{\#}$ and $I^{\#}$ as

$$S^{\#} = \frac{B + (B\lambda_2 - \mu - \vartheta - \pi - \lambda_1)\, I^{\#} - \lambda_2\,(\mu+\vartheta+\pi)\left(I^{\#}\right)^2}{\mu\,(1+\lambda_2 I^{\#})},$$

and $I^{\#}$ satisfies the fourth order equation

$$H_1\left(I^{\#}\right)^4 + H_2\left(I^{\#}\right)^3 + H_3\left(I^{\#}\right)^2 + H_4\left(I^{\#}\right) + H_5 = 0, \tag{2.4}$$

where coefficients are demonstrated by

$$\begin{aligned}
H_1 &= \theta_2(\lambda_2)^2\theta_1(\mu+\vartheta+\pi)^2,\\
H_2 &= \theta_2\lambda_2\theta_1\,(\mu+\vartheta+\pi)\,(\mu+\vartheta+\pi+\lambda_1)\\
&\quad + \lambda_2\,(\mu+\vartheta+\pi)\left(-\lambda_2\theta_1\,(\mu+\vartheta+\pi) + \theta_2\mu\lambda_2\right.\\
&\quad \left. + \theta_2\theta_1\,(B\lambda_2 - \mu - \vartheta - \pi - \lambda_1)\right)\\
&\quad + B(\lambda_2)^2\,(\mu+\vartheta+\pi),\\
H_3 &= (\mu+\vartheta+\pi+\lambda_1)\left(-\lambda_2\theta_1\,(\mu+\vartheta+\pi)\right.\\
&\quad \left. + \theta_2\mu\lambda_2 + \theta_2\theta_1\left(B\lambda_2 - \mu - \vartheta - \pi - \lambda_1\right)\right) + \lambda_2\,(\mu+\vartheta+\pi)\\
&\quad \times\left(\mu\lambda_2 + \theta_1\,(B\lambda_2 - \mu - \vartheta - \pi - \lambda_1) + \theta_2\left(\mu + \theta_1 B\right)\right)\\
&\quad - B\lambda_2\,(B\lambda_2 - 2\mu - 2\vartheta - 2\pi - \lambda_1),\\
H_4 &= (\mu+\vartheta+\pi+\lambda_1)\left(\mu\lambda_2 + \theta_1\,(B\lambda_2 - \mu - \vartheta - \pi - \lambda_1)\right.\\
&\quad \left. + \theta_2\mu + \theta_2\theta_1 B\right) + \lambda_2\,(\mu+\vartheta+\pi)\,(\mu+\theta_1 B)\\
&\quad - \beta\,(2B\lambda_2 - \mu - \vartheta - \pi - \lambda_1),\\
H_5 &= (\mu+\vartheta+\pi+\lambda_1)\,(\mu+\theta_1 B)\,(1-\Re_0).
\end{aligned}$$

Using Descartes' rule of signs [29], the biquadratic equation (2.4) has a unique positive real root $I^{\#}$ if any of the following is true:

i.
$$H_1 > 0,\; H_2 < 0,\; H_3 < 0,\; H_4 > 0,\; and\; H_5 < 0.$$

ii.
$$H_1 > 0,\; H_2 > 0,\; H_3 < 0,\; H_4 < 0,\; and\; H_5 < 0.$$

iii.

$$H_1 > 0,\ H_2 > 0,\ H_3 > 0,\ H_4 < 0,\ \textit{and}\ H_5 < 0.$$

iv.

$$H_1 > 0,\ H_2 > 0,\ H_3 > 0,\ H_4 > 0,\ \textit{and}\ H_5 < 0.$$

The value of $S^{\#}$ can be deduced from a unique $I^{\#}$ that exists if any of the previously listed conditions are satisfied. This suggests that a distinct endemic point of equilibrium $E\left(S^{\#}, I^{\#}\right)$ exists.

2.5. Stability analysis

To conduct a stability study at equilibrium points for system (2.1), the methodology outlined in [26] will be applied. Consider the system

$$\begin{cases} S_t - \tau_1 \Delta S = (1-\rho)\delta N - \dfrac{\beta SI}{(1+\theta_1 S)(1+\theta_2 I)} - \mu S, \\ I_t - \tau_2 \Delta I = \dfrac{\beta SI}{(1+\theta_1 S)(1+\theta_2 I)} - \dfrac{\lambda_1 I}{1+\lambda_2 I} - (\mu + \vartheta + \pi) I. \end{cases}$$

Using the Jacobian matrix approach, the system's characteristic equation at DFE point $E_0\left(\frac{B}{\mu}, 0\right)$ is obtained by

$$(\Gamma + \mu)\left(\Gamma + \mu + \vartheta + \pi + \lambda_1 - \frac{\beta B}{(\mu + \theta_1 B)}\right) = 0,$$

implies that

$$(\Gamma + \mu)\left(\Gamma + (1 - \Re_0)\right).$$

Therefore, roots are

$$\Gamma_1 = -\mu,\ \ \Gamma_2 = -\left(1 - \Re_0\right). \tag{2.5}$$

It is evident from equation (2.5) that only if $\Re_0 < 1$ holds, both eigenvalues for the characteristic equation corresponding to the system (2.1) at DFE point $E_0\left(\frac{B}{\mu}, 0\right)$ will be negative. As a result, we conclude:

Theorem 2.1 *If $\Re_0$ is less than 1, the DFE point $E_0\left(\frac{B}{\mu}, 0\right)$ is locally asymptotically stable; if $\Re_0$ is greater than 1, E_0 is unstable.*

The local stability analysis is now carried out at the endemic point of equilibrium $E\left(S^{\#}, I^{\#}\right)$. At the endemic point of equilibrium $E\left(S^{\#}, I^{\#}\right)$, the characteristic equation for system (2.1) is defined by

$$\Gamma^2 + p_0\Gamma + q_0 + (p_1\Gamma + q_1) = 0,$$

where

$$\begin{aligned} p_0 &= (2\mu + \vartheta + \pi) + \frac{\lambda_1}{\left(1 + \lambda_2 I^{\#}\right)^2}, \\ q_0 &= \mu\left((\mu + \vartheta + \pi) + \frac{\lambda_1}{\left(1 + \lambda_2 I^{\#}\right)^2}\right), \\ p_1 &= \frac{\beta}{(1+\theta_1 S^{\#})(1+\theta_2 I^{\#})}\left[\frac{I^{\#}}{(1+\theta_1 S^{\#})} - \frac{S^{\#}}{(1+\theta_2 I^{\#})}\right], \\ q_1 &= \frac{\beta I^{\#}}{(1+\theta_1 S^{\#})^2(1+\theta_2 I^{\#})}\left[(\mu + \vartheta + \pi) + \frac{\lambda_1}{\left(1 + \lambda_2 I^{\#}\right)^2}\right] \\ &\quad - \frac{\mu\beta S^{\#}}{(1+\theta_1 S^{\#})(1+\theta_2 I^{\#})^2}. \end{aligned}$$

Theorem 2.2 *If* $\frac{S^{\#}}{I^{\#}} \leq \frac{(1+\theta_2 I^{\#})}{(1+\theta_1 S^{\#})}$ *is satisfied, then the endemic point of equilibrium* $E\left(S^{\#}, I^{\#}\right)$ *has local asymptotic stability.*

Proof: Take the system's (2.1) characteristic equation into consideration at EE point $E\left(S^{\#}, I^{\#}\right)$

$$\Gamma^2 + p_0\Gamma + q_0 + (p_1\Gamma + q_1) = 0,$$

where the parameter values match the previously stated values.

Anyone can readily demonstrate that if $\frac{S^{\#}}{I^{\#}} \leq \frac{(1+\theta_2 I^{\#})}{(1+\theta_1 S^{\#})}$ holds, then

$$p_0 + p_1 = (2\mu + \vartheta + \pi) + \frac{\lambda_1}{(1+\lambda_2 I^{\#})^2} + \frac{\beta}{(1+\theta_1 S^{\#})(1+\theta_2 I^{\#})}\left[\frac{I^{\#}}{(1+\theta_1 S^{\#})} - \frac{S^{\#}}{(1+\theta_2 I^{\#})}\right] > 0,$$

and,

$$\begin{aligned} q_0 + q_1 &= \mu\left((\mu+\vartheta+\pi) + \frac{\lambda_1}{(1+\lambda_2 I^{\#})^2}\right) \\ &+ \frac{\beta I^{\#}}{(1+\theta_1 S^{\#})^2(1+\theta_2 I^{\#})}\left[(\mu+\vartheta+\pi) + \frac{\lambda_1}{(1+\lambda_2 I^{\#})^2}\right] \\ &- \frac{\mu\beta S^{\#}}{(1+\theta_1 S^{\#})(1+\theta_2 I^{\#})^2} \\ &= \mu\left((\mu+\vartheta+\pi) + \frac{\lambda_1}{(1+\lambda_2 I^{\#})^2}\right) \\ &+ \frac{\beta I^{\#}}{(1+\theta_1 S^{\#})^2(1+\theta_2 I^{\#})}\left[(\vartheta+\pi) + \frac{\lambda_1}{(1+\lambda_2 I^{\#})^2}\right] \\ &+ \frac{\beta\mu}{(1+\theta_1 S^{\#})(1+\theta_2 I^{\#})}\left[\frac{I^{\#}}{(1+\theta_1 S^{\#})} - \frac{S^{\#}}{(1+\theta_2 I^{\#})}\right] > 0. \end{aligned}$$

Accordingly, the EE point $E\left(S^{\#}, I^{\#}\right)$ of the system (2.1) meets the Routh-Hurwitz criterion's definition of being locally asymptotically stable. □

3. Numerical simulation and result discussion

Consider the system of equations (1.6)

$$\begin{cases} S_t - \tau_1\Delta S = (1-\rho)\delta N - \dfrac{\beta SI}{(1+\theta_1 S)(1+\theta_2 I)} - \mu S, \\ I_t - \tau_2\Delta I = \dfrac{\beta SI}{(1+\theta_1 S)(1+\theta_2 I)} - \dfrac{\lambda_1 I}{1+\lambda_2 I} - (\mu+\vartheta+\pi)I, \\ R_t - \tau_3\Delta R = \dfrac{\lambda_1 I}{1+\lambda_2 I} + \pi I + \rho\delta N - \mu R, \end{cases}$$

Using the procedure described in [6], this can be expressed as

$$\begin{aligned} \frac{\partial S}{\partial t} &= (1-\rho)\delta N - \frac{\beta SI}{(1+\theta_1 S)(1+\theta_2 I)} - \mu S + \tau_1\frac{\partial^2 S}{\partial\omega^2}, \\ \frac{\partial I}{\partial t} &= \frac{\beta SI}{(1+\theta_1 S)(1+\theta_2 I)} - \frac{\lambda_1 I}{1+\lambda_2 I} - (\mu+\vartheta+\pi)I + \tau_2\frac{\partial^2 S}{\partial\omega^2}, \\ \frac{\partial R}{\partial t} &= \frac{\lambda_1 I}{1+\lambda_2 I} + \pi I + \rho\delta N - \mu R + \tau_3\frac{\partial^2 R}{\partial\omega^2}. \end{aligned}$$

We use the same initial and boundary conditions as those specified in the system (1.6) to simulate the model in order to analyse the impact of diffusive rate.

The *pdepe* solver for the system of partial differential equations in $MATLAB\ R2017b$ has been used to perform the numerical simulation. The following tested values dataset of parameters from the published literature [16,17] have been used for simulation. Figure 1 depicts the dynamical behaviour of

Table 1: Parameters value used for numerical simulation.

Parameters	**Values**	**Dimensions**
N	1	individual per time unit
$\tau_1 = \tau_2 = \tau_3$	0.001	$(\text{individual per time unit})^{-1}$
ρ	0.65	$(\text{individual per time unit})^{-1}$
δ	0.025	$(\text{individual per time unit})^{-1}$
β	0.003	$(\text{per time unit})^{-1}$
θ_1	0.005	$(\text{per time unit})^{-1}$
θ_2	0.005	$(\text{per time unit})^{-1}$
μ	0.003	$(\text{per time unit})^{-1}$
λ_1	0.01	$(\text{per time unit})^{-1}$
λ_2	0.04	$(\text{per time unit})^{-1}$
ϑ	0.001	$(\text{per time unit})^{-1}$
π	0.001	$(\text{per time unit})^{-1}$

susceptible, infected and recovered population using the parametric parameters taken from the published literature listed in Table 1. Figure 1 shows a diffusion rate of 0.01; however, Figure 2 shows the dynamical behaviour of susceptible, infected, and recovered populations with an enhanced diffusion rate of 0.1. This demonstrates unequivocally that when the diffusion rate rises, the susceptible and infected population declines more quickly, while the recovered population grows more quickly in terms of both space and time. For susceptible and infected populations with varying diffusion rates, Figures 3 and 4 show a similar pattern. A higher diffusion rate causes a faster decline in both the susceptible and infected populations.

Since the susceptible population in our primary model (1.6) depends on three parameters: vaccination, diffusion coefficient and incident rate, thus, Figure 5$(a-c)$ demonstrates the behaviour of susceptible population for varying incident rate, vaccination rate and diffusion coefficient, respectively, for fixed spatial value $\omega = 0.25$.

Figure 6(a) shows the impact of recovery rate on infected population, and Figure 6(b) shows a $2D$ graph of the infected population over time for various spatial variable values. The behaviour of infected people with varying diffusion coefficients is shown in Figure 6(c). Figure 7 shows how vaccinations affect recovered people at different levels. This indicates that the faster the population gets vaccinated, the faster it will recover.

4. Conclusion and Future Direction

This study proposed a SIR epidemic model with diffusion. This research employed a nonlinear treatment rate, which is regarded as Holling type II, and a nonlinear infection incidence rate, which is regarded as Crowley–Martin type. A thorough mathematical investigation of the proposed model has been carried out. First, it has been established that the set of solutions is bounded and non-negative. All potentialities for the existence of endemic and disease-free equilibrium points have also been examined. Examining the model's stability at disease-free equilibrium, it was found to be locally asymptotically stable when $\Re_0 < 1$ and unstable when $\Re_0 > 1$. The disease endemic equilibrium is known to exist and stability has been demonstrated under specific circumstances. It is evident that when the fundamental reproduction number is larger than one, the infection will continue to exist in the community, and when it is less than one, the sickness will cease to exist. Further, To observe the impacts of diffusion, cure rate, limitation rate in accessible treatment, and the degrees of inhibition accepted by susceptible and infected individuals, simulations have been conducted. The *pdepe* solver for the system of partial differential

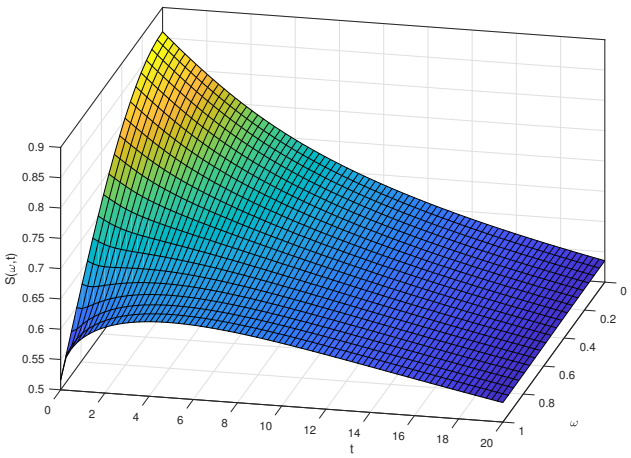

(a)

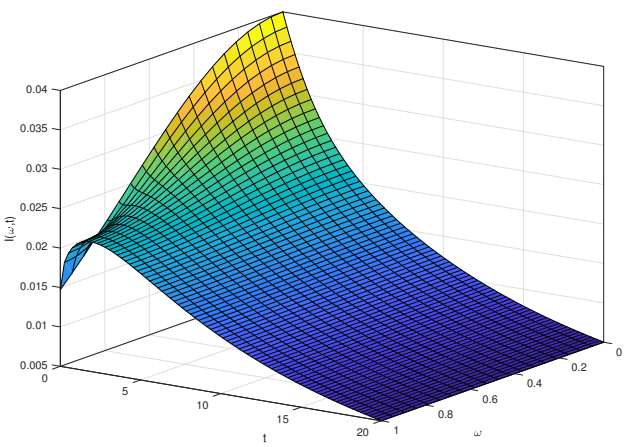

(b)

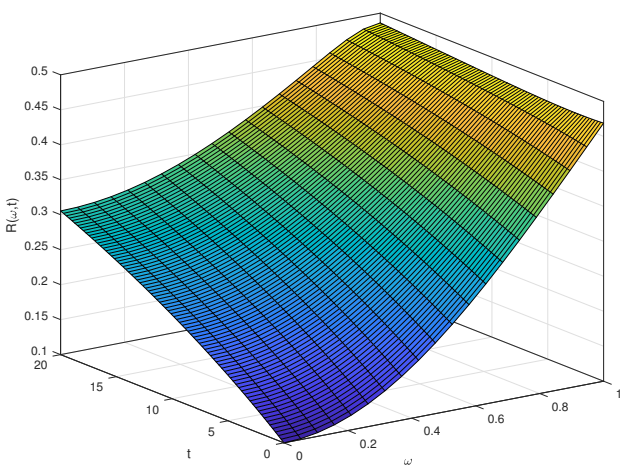

(c)

Figure 1: Output in terms of graph for susceptible, infected, and recovered populations using the parametric values given in Table 1 according to time and location.

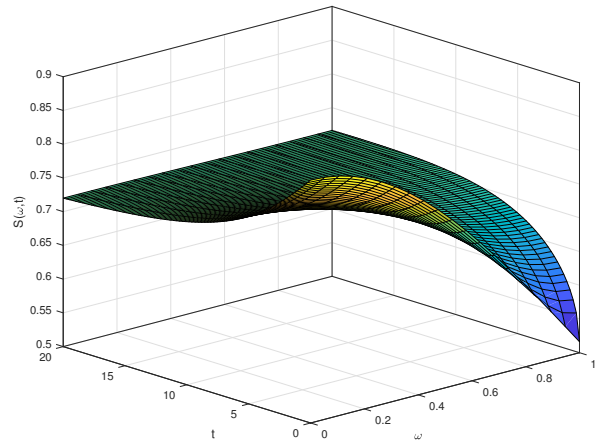

(a)

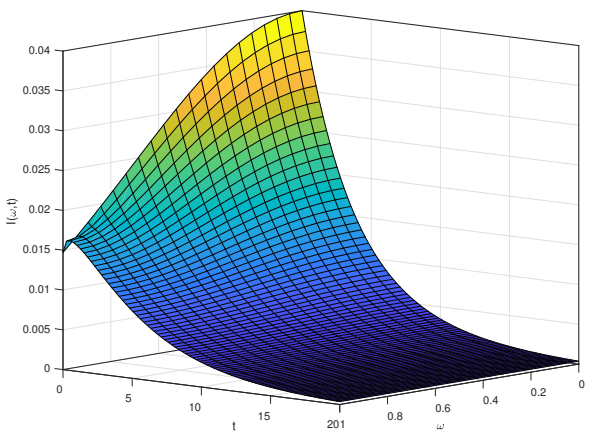

(b)

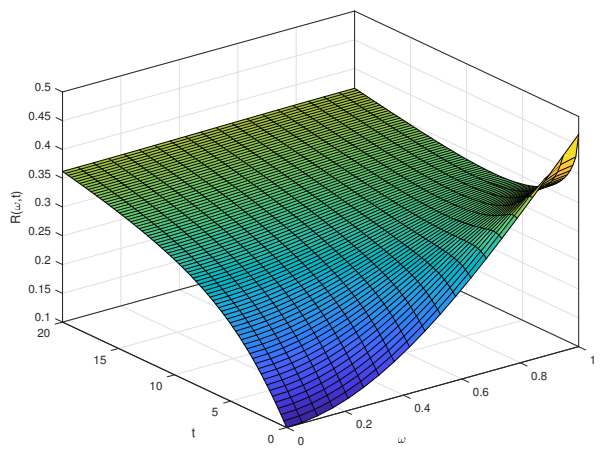

(c)

Figure 2: Output in terms of graph for susceptible, infected, and recovered populations using the parametric values given in Table 1 and diffusion coefficients as $\tau_1 = \tau_2 = \tau_3 = 0.1$

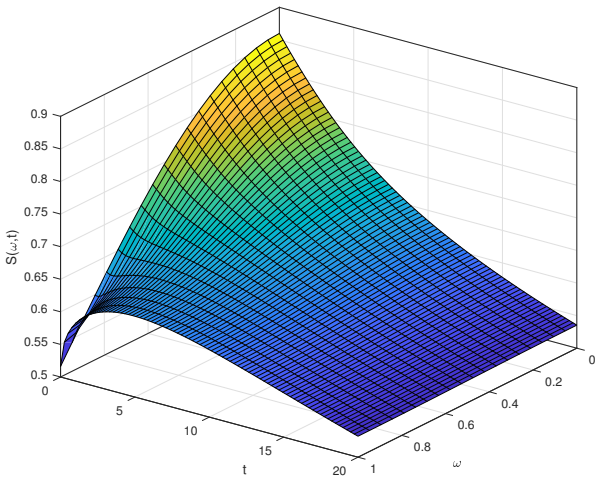

(a)

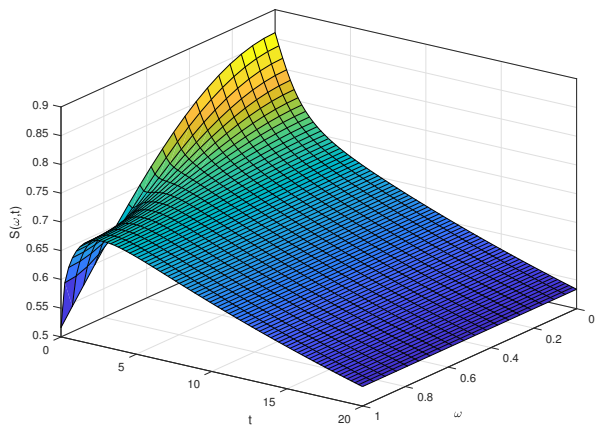

(b)

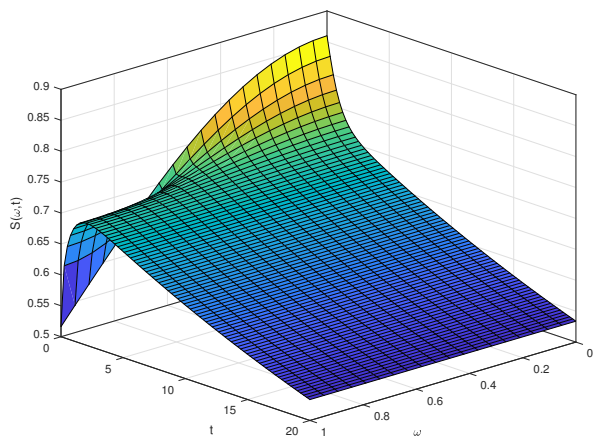

(c)

Figure 3: Graphical output showing the effect of diffusion coefficient on people who are susceptible at (a) $\tau_1 = 0.001$ (b) $\tau_1 = 0.01$ (c) $\tau_1 = 0.1$.

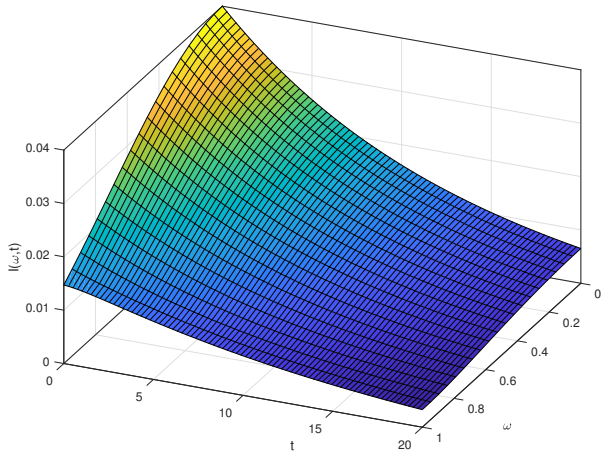

(a)

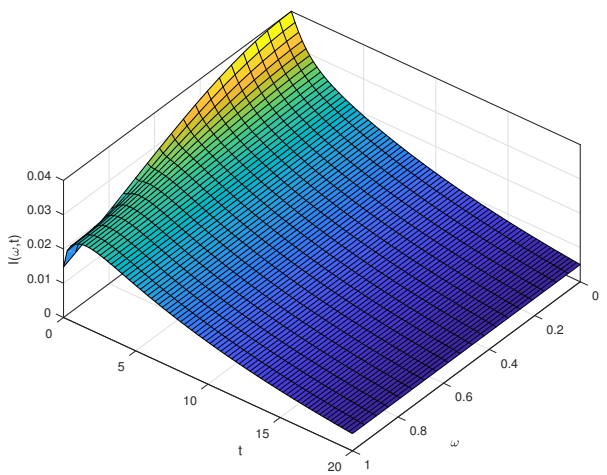

(b)

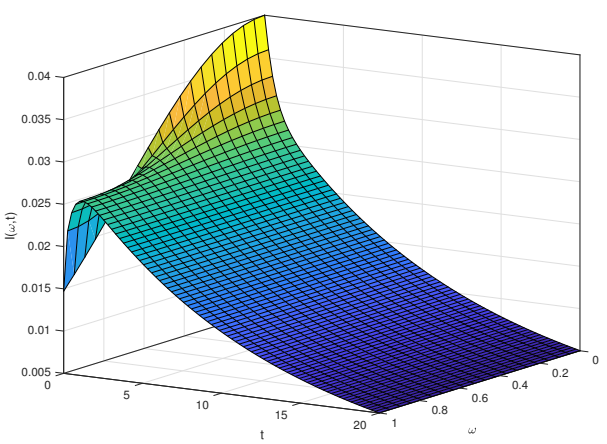

(c)

Figure 4: Graphical output showing the impact of diffusion coefficient on people who are infected at (a) $\tau_2 = 0.001$ (b) $\tau_2 = 0.01$ (c) $\tau_2 = 0.1$.

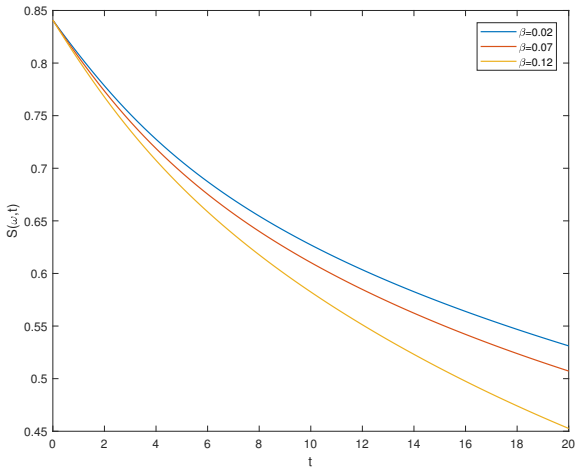

(a)

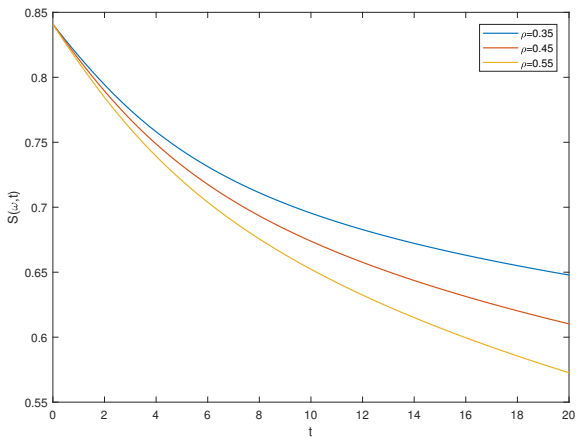

(b)

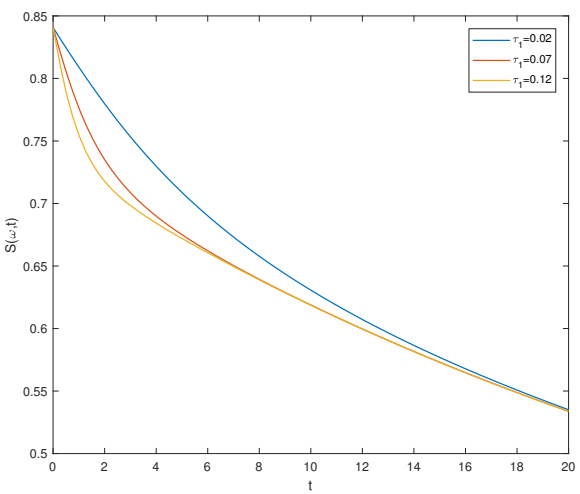

(c)

Figure 5: Graphical outputs showing the effect of incidence rate, vaccination ratio and diffusion coefficient on people who are susceptible at (a) β (b) ρ (c) $\tau_1 = 0.001, 0.01, 0.1$.

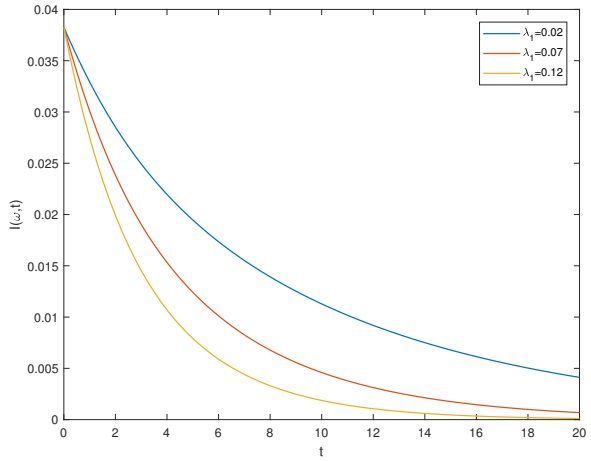

(a)

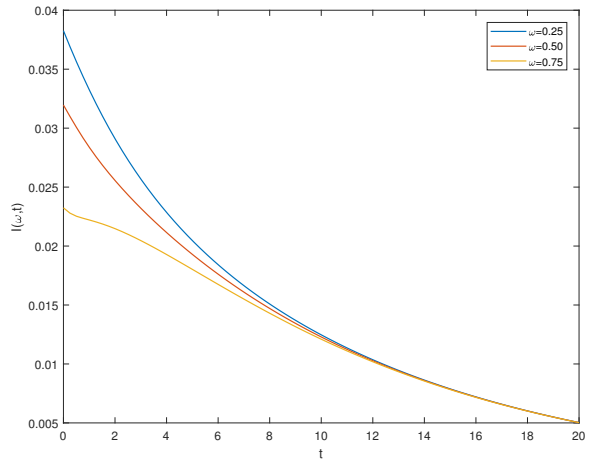

(b)

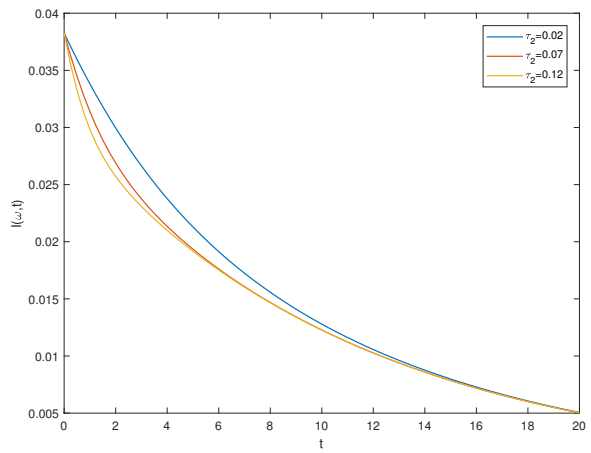

(c)

Figure 6: Graphical outputs showing the effect of recovery rate, location space and diffusion coefficient on people who are infected at (a) λ (b) ω (c) $\tau_2 = 0.001, 0.01, 0.1$.

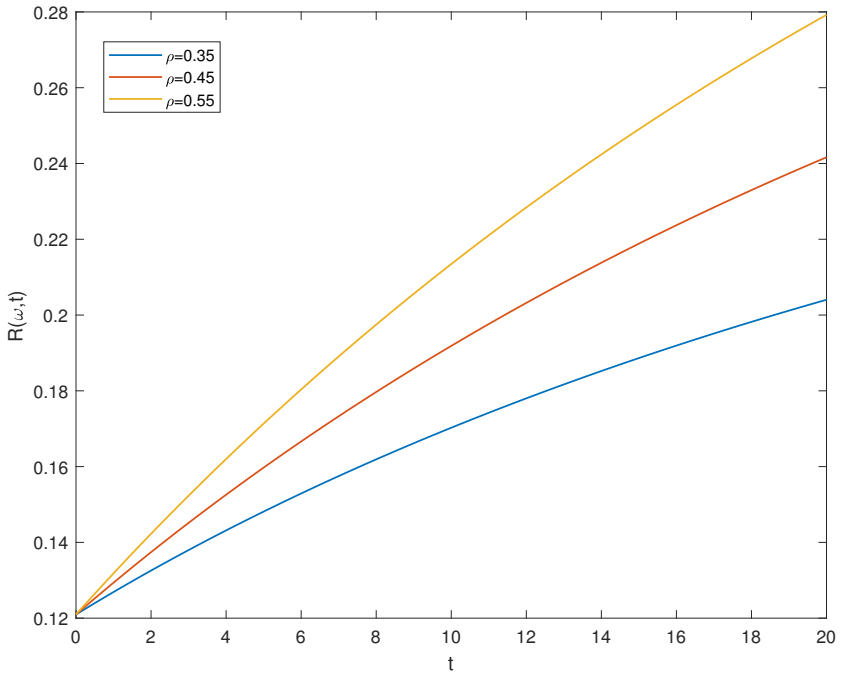

Figure 7: Graphical output illustrating the effects of vaccinations at different levels on people who have recovered

equations in *MATLAB R2017b* has been used to perform the numerical simulation. Since the entire population is regarded as one, representing 100% of the population, a graph indicator value of 0.3 will reflect 30% of the total population. The model's numerical simulation demonstrates that when the rate of transmission increases, the infection will increase else decrease due to treatment availability. Additionally, when the degree of inhibition adopted by susceptible and infectious individuals increases, a decrease in infection is being noted. Moreover, the effect of the diffusion coefficient has been observed through graphical representations which indicate that as the diffusion coefficient increases, the susceptible and infected population decreases rapidly while the recovered population grows more quickly.

Our next research will concentrate on analysing our model's stability using a variety of nonlinear treatment function types and incident rates. For this study, we will also consider derivatives of the fractional kind and determine their benefits and drawbacks.

Declarations

Availability of data and materials

Not applicable.

Competing interests

The authors declare that they have no competing interests.

Funding

Not Applicable

4.1. Authors' contributions

Each author contributed equally to the work.

4.2. Acknowledgments

Authors are thankful to the reviewers for their constructive comments to improve this paper.

References

1. R Agarwal, MP Yadav, RP Agarwal, and R Goyal. Analytic solution of fractional advection dispersion equation with decay for contaminant transport in porous media. *Matematički Vesnik*, 71(1-2):5–15, 2019.

2. Ritu Agarwal, Mahaveer Prasad Yadav, and Ravi P Agarwal. Space time fractional boussinesq equation with singular and non singular kernels. *International Journal of Dynamical Systems and Differential Equations*, 10(5):415–426, 2020.

3. Ghaliah Alhamzi, Badr Saad T Alkahtani, Ravi Shanker Dubey, and Mati ur Rahman. Global piecewise analysis of hiv model with bi-infectious categories under ordinary derivative and non-singular operator with neural network approach. *CMES-Computer Modeling in Engineering and Sciences*, 142(1):609–633, 2024.

4. Linda JS Allen, Ben M Bolker, Yuan Lou, and Andrew L Nevai. Asymptotic profiles of the steady states for an sis epidemic reaction-diffusion model. 2008.

5. R Anderson. *Infectious diseases of humans: dynamics and control*. Cambridge Univer-sity Press, 1991.

6. Settapat Chinviriyasit and Wirawan Chinviriyasit. Numerical modelling of an sir epidemic model with diffusion. *Applied Mathematics and Computation*, 216(2):395–409, 2010.

7. Philip H Crowley and Elizabeth K Martin. Functional responses and interference within and between year classes of a dragonfly population. *Journal of the North American Benthological Society*, 8(3):211–221, 1989.

8. Balram Dubey, Atasi Patra, PK Srivastava, and Uma S Dubey. Modeling and analysis of an seir model with different types of nonlinear treatment rates. *Journal of Biological Systems*, 21(03):1350023, 2013.

9. Preeti Dubey, Balram Dubey, and Uma S Dubey. An sir model with nonlinear incidence rate and holling type iii treatment rate. In *Applied Analysis in Biological and Physical Sciences: ICMBAA, Aligarh, India, June 2015*, pages 63–81. Springer, 2016.

10. Abba B Gumel, C Connell McCluskey, and James Watmough. An sveir model for assessing potential impact of an imperfect anti-sars vaccine. 2006.

11. Daniel Henry. *Geometric theory of semilinear parabolic equations*, volume 840. Springer, 2006.

12. Herbert W Hethcote. Qualitative analyses of communicable disease models. *Mathematical biosciences*, 28(3-4):335–356, 1976.

13. SAA Karim and R Razali. A proposed mathematical model of influenza a, h1n1 for malaysia. *Journal of Applied Sciences*, 11(8):1457–1460, 2011.

14. William Ogilvy Kermack and Anderson G McKendrick. A contribution to the mathematical theory of epidemics. *Proceedings of the royal society of london. Series A, Containing papers of a mathematical and physical character*, 115(772):700–721, 1927.

15. William Ogilvy Kermack and Anderson G McKendrick. Contributions to the mathematical theory of epidemics. ii.—the problem of endemicity. *Proceedings of the Royal Society of London. Series A, containing papers of a mathematical and physical character*, 138(834):55–83, 1932.

16. Abhishek Kumar and Nilam. Stability of a time delayed sir epidemic model along with nonlinear incidence rate and holling type-ii treatment rate. *International Journal of Computational Methods*, 15(06):1850055, 2018.

17. Abhishek Kumar and Nilam. Dynamical model of epidemic along with time delay; holling type ii incidence rate and monod–haldane type treatment rate. *Differential Equations and Dynamical Systems*, 27:299–312, 2019.

18. Abhishek Kumar, Nilam, and Raj Kishor. A short study of an sir model with inclusion of an alert class, two explicit nonlinear incidence rates and saturated treatment rate. *SeMA Journal*, 76:505–519, 2019.

19. Michael Y Li, John R Graef, Liancheng Wang, and János Karsai. Global dynamics of a seir model with varying total population size. *Mathematical biosciences*, 160(2):191–213, 1999.

20. Mingming Li and Xianning Liu. An sir epidemic model with time delay and general nonlinear incidence rate. In *Abstract and Applied Analysis*, volume 2014, page 131257. Wiley Online Library, 2014.

21. Manisha Meena, Mridula Purohit, Sunil Dutt Purohit, Kottakkaran Sooppy Nisar, et al. A novel investigation of the hepatitis b virus using a fractional operator with a non-local kernel. *Partial Differential Equations in Applied Mathematics*, 8:100577, 2023.

22. Kanak Modi, Laxmikant Umate, Kiran Makade, Ravi Shanker Dubey, and Pankaj Agarwal. Simulation based study for estimation of covid-19 spread in india using seir model. *Journal of Interdisciplinary Mathematics*, 24(2):245–258, 2021.

23. Murray H Protter and Hans F Weinberger. *Maximum principles in differential equations*. Springer Science & Business Media, 2012.

24. Xiangyun Shi, Xueyong Zhou, and Xinyu Song. Analysis of a stage-structured predator-prey model with crowley-martin function. *Journal of Applied Mathematics and Computing*, 36(1):459–472, 2011.

25. Mansour Shrahili, Ravi Shanker Dubey, and Ahmed Shafay. Inclusion of fading memory to banister model of changes in physical condition. *Discrete and Continuous Dynamical Systems-S*, 13(3):881–888, 2020.

26. Sirachat Tipsri and Wirawan Chinviriyasit. Stability analysis of seir model with saturated incidence and time delay. *International Journal of Applied Physics and Mathematics*, 4(1):42, 2014.

27. Pauline Van den Driessche and James Watmough. Reproduction numbers and sub-threshold endemic equilibria for compartmental models of disease transmission. *Mathematical biosciences*, 180(1-2):29–48, 2002.

28. Wendi Wang and Shigui Ruan. Bifurcations in an epidemic model with constant removal rate of the infectives. *Journal of Mathematical Analysis and Applications*, 291(2):775–793, 2004.

29. Xiaoshen Wang. A simple proof of descartes's rule of signs. *The American Mathematical Monthly*, 111(6):525–526, 2004.

30. Rui Xu and Zhien Ma. Stability of a delayed sirs epidemic model with a nonlinear incidence rate. *Chaos, Solitons & Fractals*, 41(5):2319–2325, 2009.

31. Mahaveer Prasad Yadav and Ritu Agarwal. Numerical investigation of fractional-fractal boussinesq equation. *Chaos: An Interdisciplinary Journal of Nonlinear Science*, 29(1), 2019.

32. Xu Zhang and Xianning Liu. Backward bifurcation of an epidemic model with saturated treatment function. *Journal of mathematical analysis and applications*, 348(1):433–443, 2008.

33. Zhang Zhonghua and Suo Yaohong. Qualitative analysis of a sir epidemic model with saturated treatment rate. *Journal of Applied Mathematics and Computing*, 34:177–194, 2010.

34. Linhua Zhou and Meng Fan. Dynamics of an sir epidemic model with limited medical resources revisited. *Nonlinear Analysis: Real World Applications*, 13(1):312–324, 2012.

Kuldeep Malik,
School of Liberal Studies,
Dr. B. R. Ambedkar University Delhi, Delhi-110006,
India.
E-mail address: malik.kuldep@gmail.com

and

Pranay Goswami,
School of Liberal Studies,
Dr. B. R. Ambedkar University Delhi, Delhi-110006,
India.
E-mail address: pranaygoswami83@gmail.com, pranay@aud.ac.in

and

Vikas Yadav,
Department of Mathematics,
Vivekananda Global University, Jaipur,
India.
E-mail address: vikashyadav016190@gmail.com